Medullary thymic epithelial NF–kB-inducing kinase (NIK)/IKKα pathway shapes autoimmunity and liver and lung homeostasis in mice

Hong Shen[a], Yewei Ji[a], Yi Xiong[a], Hana Kim[a], Xiao Zhong[a], Michelle G. Jin[a], Yatrik M. Shah[a], M. Bishr Omary[a,1], Yong Liu[b], Ling Qi[a], and Liangyou Rui[a,c,2]

[a]Department of Molecular and Integrative Physiology, University of Michigan Medical School, Ann Arbor, MI 48109; [b]College of Life Sciences, The Institute for Advanced Studies, Wuhan University, 430072 Wuhan, China; and [c]Department of Internal Medicine, University of Michigan Medical School, Ann Arbor, MI 48109

Edited by Sankar Ghosh, Columbia University Medical Center, New York, NY, and accepted by Editorial Board Member Ruslan Medzhitov August 5, 2019 (received for review January 22, 2019)

Aberrant T cell development is a pivotal risk factor for autoimmune disease; however, the underlying molecular mechanism of T cell overactivation is poorly understood. Here, we identified NF–κB-inducing kinase (NIK) and IkB kinase α (IKKα) in thymic epithelial cells (TECs) as essential regulators of T cell development. Mouse TEC-specific ablation of either NIK or IKKα resulted in severe T cell-mediated inflammation, injury, and fibrosis in the liver and lung, leading to premature death within 18 d of age. NIK or IKKα deficiency abrogated medullary TEC development, and led to breakdown of central tolerance, production of autoreactive T cells, and fatal autoimmune destruction in the liver and lung. TEC-specific ablation of NIK or IKKα also impaired thymic T cell development from the double-negative through the double-positive stages and inhibited peripheral B cell development. These results unravel a hitherto unrecognized essential role of TEC-intrinsic NIK and IKKα pathways in autoimmunity and T cell-instigated chronic liver and lung diseases.

NIK and IKKalpha | autoimmune disease | thymic epithelial cells | liver disease | lung disease

Liver and lung diseases are an important cause of mortality and morbidity and are fueled by inflammation (1–3). Recent research highlights a pathogenic contribution of adaptive immunity, particularly T cell-triggered destruction, to liver and/or lung diseases (1–3); however, the underlying mechanism of T cell activation is poorly understood. Naïve T cell development is controlled by thymic epithelial cells (TECs). Cortical TECs (cTECs) control thymic seeding of lymphocyte stem cells and subsequent thymocyte proliferation and differentiation; medullary TECs (mTECs) are responsible for negative selection and establishment of central tolerance to remove autoreactive T cells (4). Reciprocally, developing thymocytes also profoundly influence the growth and differentiation of cTECs and mTECs through secreting various cytokines, including receptor activator of NF-κB ligand (RANKL), lymphotoxin β (LTβ), and CD40L (4). Accordingly, ablation of RANKL, LTβ, CD40L, or their cognate receptors blocks mTEC development, resulting in autoimmune disease (5–9). However, mTEC-intrinsic pathways mediating thymocyte–mTEC crosstalk remain elusive.

RANKL, LTβ, and CD40L activate the noncanonical NF–kB2 pathway in immune cells (10). These cytokines stimulate NF–κB-inducing kinase (NIK), also known as MAP3K14. NIK phosphorylates and activates IkB kinase α (IKKα), also called CHUK. IKKα in turn phosphorylates NF–kB2 precursor p100, generating mature p52 that binds to RelB and activates target genes. Global inactivation of NIK abrogates thymic medullary development in mice, leading to autoimmune disease (11, 12). Importantly, human $NIK^{Pro565Arg}$ and $NIK^{Val345Met}$ variants are linked to profound immune dysfunctions (13, 14). Thus, NIK is an essential regulator of the immune system in both mice and humans. However, NIK target cells remain elusive. We postulated that mTEC NIK/IKKα pathways might mediate thymocyte–mTEC crosstalk, shaping mTEC growth and differentiation. To test this hypothesis, we generated and characterized TEC-specific *NIK* ($NIK^{\Delta TEC}$) and *IKKα* ($IKK\alpha^{\Delta TEC}$) knockout mice. Using these mice, we firmly established a pivotal role of the mTEC-intrinsic NIK/IKKα pathway in mTEC development and establishment of central tolerance. We also unraveled mTEC–liver and mTEC–lung axes involved in liver and lung diseases.

Results

$NIK^{\Delta TEC}$ and $IKK\alpha^{\Delta TEC}$ Mice Die Prematurely. $NIK^{\Delta TEC}$ and $IKK\alpha^{\Delta TEC}$ mice were generated by crossing $NIK^{f/f}$ and $IKK\alpha^{f/f}$ mice with Foxn1–Cre drivers, respectively. $NIK^{f/f}$, $IKK\alpha^{f/f}$, and Foxn1–Cre mice were described previously (15–17). $Foxn1^{+}$ TEC progenitors are known to give rise to both cTECs and mTECs (18, 19). We confirmed that in $NIK^{\Delta TEC}$ mice, NIK was ablated specifically in TECs but not livers, lungs, spleens, kidneys, and gastrointestinal tracts (GI) (*SI Appendix*, Fig. S1 *A* and *B*). Immunoreactivity to NF–kB2 p52 (a surrogate marker for NIK activation) was high in

Significance

Aberrant T cell activation augments liver and lung diseases, increasing mortality and morbidity. T cell development is controlled by thymic epithelial cells (TECs); therefore, elucidation of TEC growth and differentiation holds a key for understanding of adaptive immunity and autoimmune disease. We found that NIK/IKKα pathways are highly activated in medullary TECs. TEC-specific ablation of NIK or IKKα blocked medullary TEC development, resulting in production of pathogenic autoreactive T cells due to breakdown of T cell central tolerance. Consequently, NIK- or IKKα-deficient mice displayed fatal autoimmune destruction of livers and lungs. This work unravels a regulation of autoimmunity by TEC-intrinsic NIK/IKKα pathways and identifies the NIK/IKKα pathway as a potential target for the treatment of chronic liver and/or lung disease.

Author contributions: H.S. and L.R. designed research; H.S., Y.J., Y.X., H.K., X.Z., and M.G.J. performed research; Y.J., Y.M.S., M.B.O., and L.Q. contributed new reagents/analytic tools; H.S., Y.J., Y.X., H.K., M.B.O., Y.L., L.Q., and L.R. analyzed data; and H.S. and L.R. wrote the paper.

The authors declare no conflict of interest.

This article is a PNAS Direct Submission. S.G. is a guest editor invited by the Editorial Board.

[1]Present address: Center for Advanced Biotechnology and Medicine, Rutgers University, Piscataway, NJ 08854.

[2]To whom correspondence may be addressed. Email: ruily@umich.edu.

This article contains supporting information online at www.pnas.org/lookup/suppl/doi:10.1073/pnas.1901056116/-/DCSupplemental.

Published online September 3, 2019.

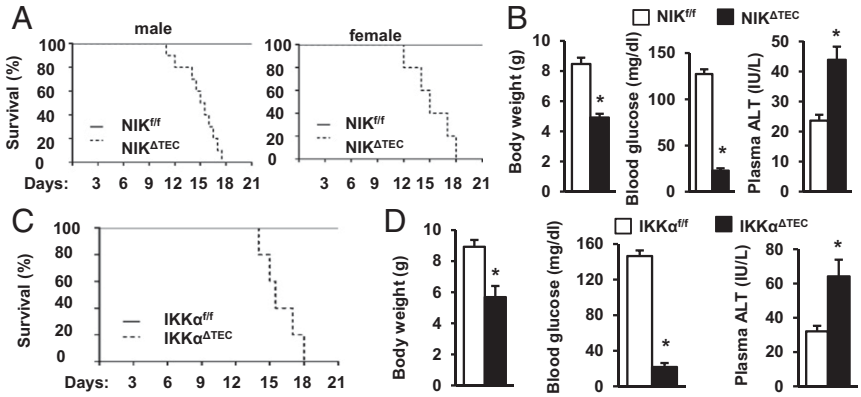

Fig. 1. TEC-specific ablation of NIK or IKKα causes hypoglycemia and premature death. (*A*) Survival rates. Male NIK$^{\Delta TEC}$, $n = 7$; male NIK$^{f/f}$, $n = 10$; female NIK$^{\Delta TEC}$, $n = 5$; female NIK$^{f/f}$, $n = 5$. (*B*) Body weight, nonfasting blood glucose, and ALT levels in males at 15 to 17 d of age. NIK$^{\Delta TEC}$, $n = 6$; NIK$^{f/f}$, $n = 7$. (*C*) Survival rates. IKKα$^{\Delta TEC}$, $n = 6$; IKKα$^{f/f}$, $n = 5$. (*D*) Body weight, nonfasting blood glucose, and plasma ALT levels in males at 15 to 17 d of age. IKKα$^{\Delta TEC}$, $n = 4$; IKKα$^{f/f}$, $n = 5$. Data are presented as mean ± SEM. *$P < 0.05$, 2-tailed unpaired Student's *t* test.

the thymic medulla of NIK$^{f/f}$ and IKKα$^{f/f}$ but not NIK$^{\Delta TEC}$ and IKKα$^{\Delta TEC}$ mice (*SI Appendix*, Fig. S1 *C* and *D*). Remarkably, NIK$^{\Delta TEC}$ male and female mice died prematurely within 18 d of age (Fig. 1*A*). NIK$^{\Delta TEC}$ pups displayed severe growth retardation and life-threatening hypoglycemia (Fig. 1*B*). The levels of plasma alanine aminotransferase (ALT), a liver injury marker,

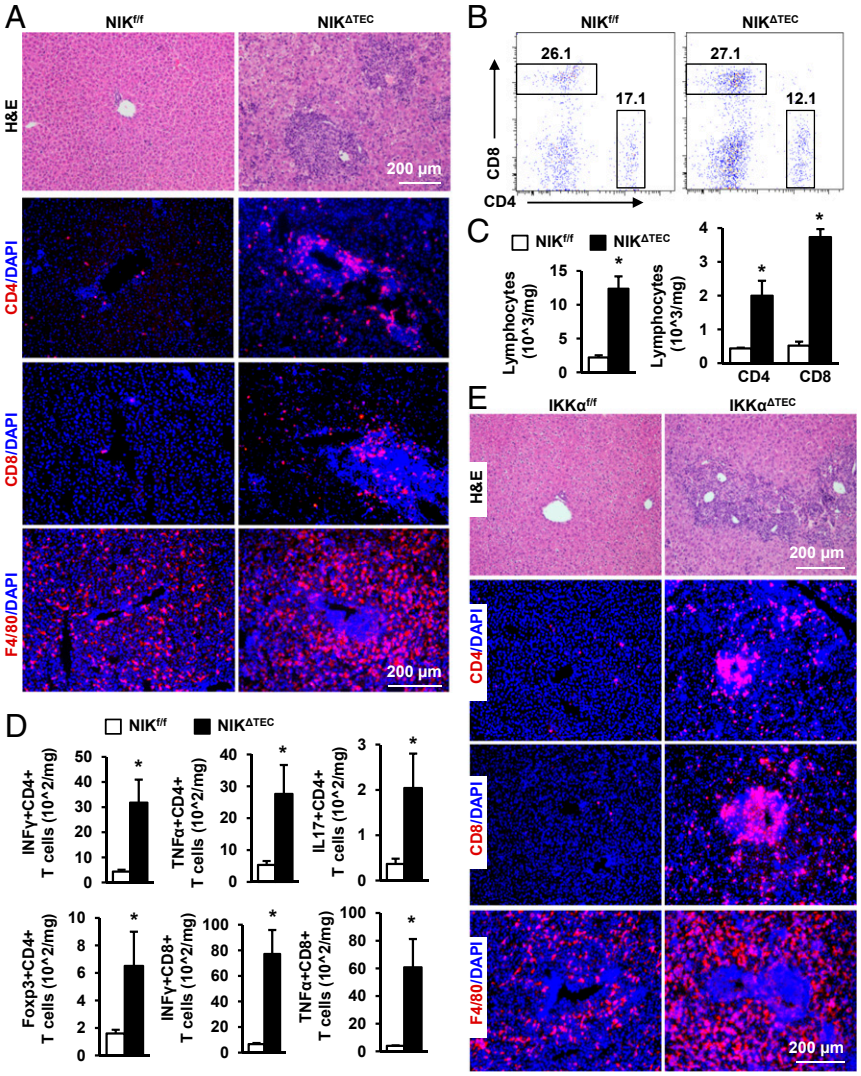

Fig. 2. NIK$^{\Delta TEC}$ and IKKα$^{\Delta TEC}$ mice develop autoimmune hepatitis. (*A* and *E*) Representative liver sections ($n = 4$ per group). (*B*) Flow cytometric plots of liver T cells. Numbers represent percentiles (normalized to CD45$^+$ lymphocytes). (*C*) Flow cytometric assessments of liver CD45$^+$ lymphocytes (normalized to liver weight). NIK$^{\Delta TEC}$, $n = 3$; NIK$^{f/f}$, $n = 3$. (*D*) Flow cytometric assessments of T cell subpopulations in males at 10 d of age. NIK$^{\Delta TEC}$, $n = 3$ to 4; NIK$^{f/f}$, $n = 4$ to 6. (*A*–*C* and *E*) Males at 15 to 17 d of age. Data are presented as mean ± SEM. *$P < 0.05$, 2-tailed unpaired Student's *t* test.

were significantly higher in NIK$^{\Delta TEC}$ mice relative to NIK$^{f/f}$ littermates (Fig. 1*B*). Likewise, IKKα$^{\Delta TEC}$ mice largely phenocopied NIK$^{\Delta TEC}$ mice (Fig. 1 *C* and *D*). These results demonstrate that TEC-intrinsic NIK and IKKα are required for postnatal survival.

NIK$^{\Delta TEC}$ and IKKα$^{\Delta TEC}$ Mice Develop Severe Autoimmune Hepatitis, Liver Injury, and Fibrosis. Impaired liver function prompted us to examine liver integrity and injury in NIK$^{\Delta TEC}$ and IKKα$^{\Delta TEC}$ mice. Strikingly, the liver was disorganized and heavily infiltrated with CD4 T cells and CD8 T cells in NIK$^{\Delta TEC}$ mice at 15 to 17 d of age (Fig. 2*A*). Flow cytometric analysis confirmed that the numbers of total lymphocytes, CD4 T cells, and CD8 T cells, but not the frequencies of CD4 and CD8 T cells (normalized to CD45$^+$ lymphocytes), in the liver were substantially higher in NIK$^{\Delta TEC}$ relative to NIK$^{f/f}$ mice (Fig. 2 *B* and *C*). In NIK$^{\Delta TEC}$ mice, liver T cells displayed activated phenotypes, expressing CD69 (*SI Appendix*, Fig. S2 *A* and *B*). Accordingly, proinflammatory INFγ$^+$CD4$^+$, TNFα$^+$CD4$^+$, IL17$^+$CD4$^+$, INFγ$^+$CD8$^+$, and TNFα$^+$CD8$^+$ subpopulations were significantly higher in NIK$^{\Delta TEC}$ than in NIK$^{f/f}$ mice (Fig. 2*D* and *SI Appendix*, Fig. S2*C*). Foxp3$^+$CD4$^+$ Treg cells were also elevated in NIK$^{\Delta TEC}$ mice (Fig. 2*D*). Likewise, IKKα$^{\Delta TEC}$ mice also developed severe autoimmune hepatitis and massive hepatic infiltrations of CD4 T cells and CD8 T cells, as assessed by immunostaining of liver sections (Fig. 2*E*). Flow cytometric analysis further confirmed that liver CD4 and CD8 T cells were not only elevated but also activated (*SI Appendix*, Fig. S2*D*). The number of liver F4/80$^+$ Kupffer cells/macrophages was also abnormally higher in both NIK$^{\Delta TEC}$ and IKKα$^{\Delta TEC}$ mice (Fig. 2 *A* and *E*). Inflammation is known to augment liver injury and fibrosis. Accordingly, the number of liver TUNEL$^+$ apoptotic cells and Sirius red$^+$ fibrosis areas were substantially higher in NIK$^{\Delta TEC}$ (relative to NIK$^{f/f}$) and IKKα$^{\Delta TEC}$ (relative to IKKα$^{f/f}$) mice (Fig. 3 *A*–*D*). The levels of cleaved caspase 3 (apoptosis marker), RIP3 (necrosis marker), and α-smooth muscle actin (αSMA, fibrosis marker) in liver extracts were also drastically higher in NIK$^{\Delta TEC}$ than in NIK$^{f/f}$ mice (Fig. 3*E*). These data unveil a TEC–liver axis involved in liver autoimmune disease.

NIK$^{\Delta TEC}$ and IKKα$^{\Delta TEC}$ Mice Develop Lung Autoimmune Disease. We next examined autoimmune inflammation in other vital organs of NIK$^{\Delta TEC}$ and IKKα$^{\Delta TEC}$ mice at 15 to 17 d of age. In NIK$^{\Delta TEC}$ mice, the lung was disrupted and heavily infiltrated with CD4 T cells, CD8 T cells, and F4/80$^+$ macrophages (Fig. 4*A*). Flow cytometric analysis confirmed that INFγ$^+$CD4$^+$, TNFα$^+$CD4$^+$, IL17$^+$CD4$^+$, INFγ$^+$CD8$^+$, and TNFα$^+$CD8$^+$ subpopulations were significantly expanded in NIK$^{\Delta TEC}$ mice compared to NIK$^{f/f}$ littermates (Fig. 4*B* and *SI Appendix*, Fig. S3 *A*–*C*). NIK$^{\Delta TEC}$ mice developed lung fibrosis, as assessed by Sirius red staining of lung sections (Fig. 4*A*). The levels of cleaved caspase 3, RIP3, and αSMA in lung extracts were drastically higher in NIK$^{\Delta TEC}$ relative to NIK$^{f/f}$ littermates (Fig. 4*C*). IKKα$^{\Delta TEC}$ mice, like NIK$^{\Delta TEC}$ mice, also developed severe lung inflammation, injury, and fibrosis (Fig. 4*D*). The levels of cleaved caspase 3, RIP3, and αSMA in both lung and liver extracts were drastically higher in IKKα$^{\Delta TEC}$ than in IKKα$^{f/f}$ mice (*SI Appendix*, Fig. S3*D*). Notably, autoimmune inflammation was mild in the kidneys and intestines of NIK$^{\Delta TEC}$ and IKKα$^{\Delta TEC}$ mice (*SI Appendix*, Fig. S4 *A* and *B*). These results uncover an unrecognized TEC–lung axis involved in lung autoimmune disease.

Peripheral B Cell Development Is Impaired in NIK$^{\Delta TEC}$ and IKKα$^{\Delta TEC}$ Mice. Considering the critical role of CD4 T cells in B cell differentiation, we assessed B cells in spleens and lymph nodes at 15 to 17 d of age. The spleens (Fig. 5*A*) and lymph nodes (*SI Appendix*, Fig. S5*A*) of NIK$^{\Delta TEC}$ mice lacked morphologically defined lymphoid follicles and germinal centers. The frequency and number of B220$^+$ B cells were dramatically lower in the spleens (Fig. 5 *B* and *C*) and lymph nodes (*SI Appendix*, Fig. S5*B*) of NIK$^{\Delta TEC}$ relative to NIK$^{f/f}$ mice. The frequency of

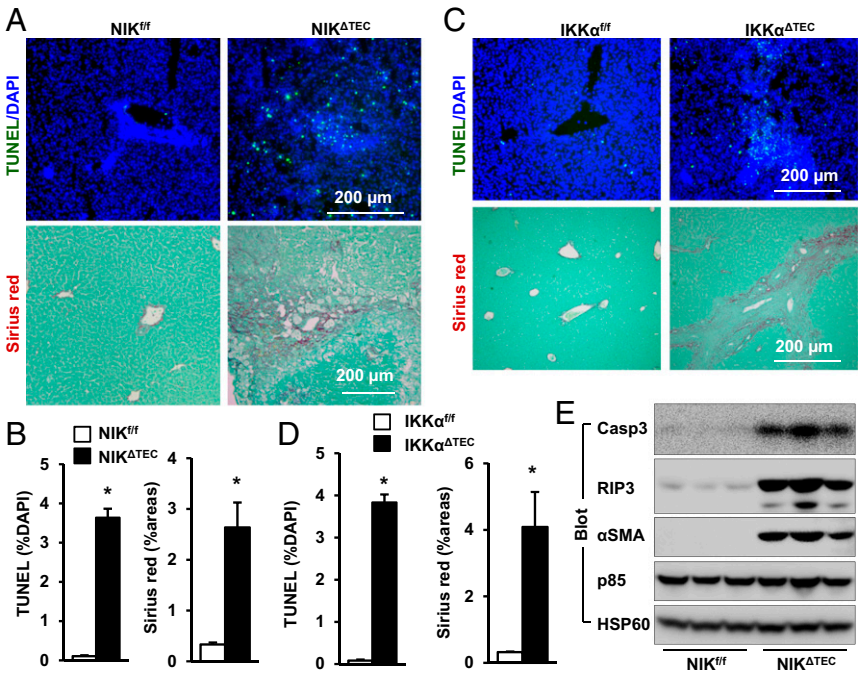

Fig. 3. NIK$^{\Delta TEC}$ and IKKα$^{\Delta TEC}$ mice develop liver injury and fibrosis. Livers were harvested from males at 15 to 17 d of age. (*A* and *C*) Representative liver sections ($n = 4$ per group). (*B* and *D*) TUNEL$^+$ apoptotic cells (normalized to total cells) and Sirius red+ areas (normalized to total view areas) in liver sections. NIK$^{\Delta TEC}$, $n = 4$; NIK$^{f/f}$, $n = 4$; IKKα$^{\Delta TEC}$, $n = 4$; IKKα$^{f/f}$, $n = 4$. (*E*) Liver extracts were immunoblotted with the indicated antibodies. Data are presented as mean ± SEM. *$P < 0.05$, 2-tailed unpaired Student's *t* test.

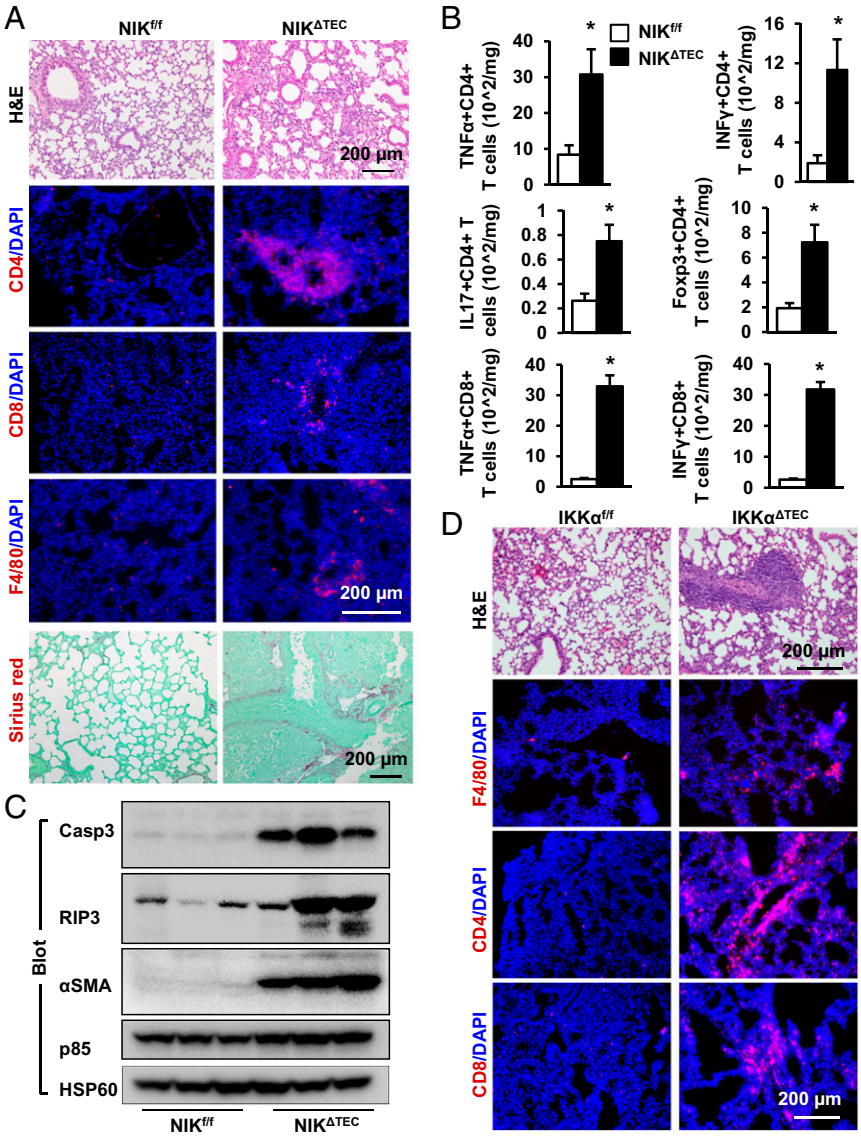

Fig. 4. NIK$^{\Delta TEC}$ and IKKα$^{\Delta TEC}$ mice develop autoimmune lung lesions. (*A* and *D*) Representative lung sections (n = 3 to 4 per group). (*B*) Flow cytometric assessments of lung T cell subpopulations in males at 10 d of age. NIK$^{\Delta TEC}$, n = 3 to 4; NIK$^{f/f}$, n = 4 to 6. (*C*) Lung extracts were immunoblotted with the indicated antibodies. (*A*, *C*, and *D*) Males at 15 to 17 d of age. Data are presented as mean ± SEM. *P < 0.05, 2-tailed unpaired Student's t test.

spleen IgM$^+$ B cells was significantly lower, while their proliferation and survival were relatively normal in NIK$^{\Delta TEC}$ mice (Fig. 5*C* and *SI Appendix*, Fig. S5*C*). These results suggest that B cell maturation is impaired in NIK$^{\Delta TEC}$ mice. Notably, spleen CD4 and CD8 T cells were also significantly lower in NIK$^{\Delta TEC}$ than in NIK$^{f/f}$ mice (Fig. 5*D*). Follicular helper (Tfh) T cells are instrumental to B cell growth and maturation, prompting us to assess CD4$^+$CXCR5$^+$PD-1$^+$ Tfh cells (20). The frequency and number of Tfh cells were significantly lower in NIK$^{\Delta TEC}$ than in NIK$^{f/f}$ littermates (Fig. 5*E* and *SI Appendix*, Fig. S5*D*). Likewise, IKKα$^{\Delta TEC}$ mice also displayed peripheral B cell deficiency, as assessed by immunostaining of spleen and lymph node sections (*SI Appendix*, Fig. S6*A*). Flow cytometric analysis confirmed that the numbers of total B cells as well as IgM$^+$ subpopulation in the spleen were lower in IKKα$^{\Delta TEC}$ than in IKKα$^{f/f}$ mice (Fig. 5*F*). The number of spleen Tfh cells was also lower in IKKα$^{\Delta TEC}$ relative to IKKα$^{f/f}$ littermates (*SI Appendix*, Fig. S6*B*). These data suggest that the TEC-intrinsic NIK/IKKα pathway promotes peripheral B cell development, presumably through Tfh and/or related CD4 T cells.

Thymocyte Development Is Impaired in NIK$^{\Delta TEC}$ Mice. Given the importance of TECs in T cell development, we examined thymocyte development stages in NIK$^{\Delta TEC}$ mice at 15 to 17 d of age. Thymus weight and total thymocyte number were dramatically lower in NIK$^{\Delta TEC}$ than in NIK$^{f/f}$ littermates (Fig. 6*A*). Flow cytometric analysis demonstrated that the frequency of CD4$^-$CD8$^-$ double-negative (DN) thymocytes was significantly higher, while the frequency of CD4$^+$CD8$^+$ double-positive (DP) thymocytes was substantially lower, in NIK$^{\Delta TEC}$ mice relative to NIK$^{f/f}$ littermates (Fig. 6 *B* and *C*). Therefore, thymocyte differentiation likely arrests between DN and DP stages. The frequency of CD25$^-$CD44$^+$ DN1 but not CD25$^+$CD44$^+$ DN2 cells was significantly higher in NIK$^{\Delta TEC}$ relative to NIK$^{f/f}$ mice (Fig. 6*D*), suggesting that DN differentiation is blocked between DN1 to DN2 stages. The frequency of CD25$^+$CD44$^-$ DN3 thymocytes was significantly lower, while DN2 frequency was relatively normal in NIK$^{\Delta TEC}$ mice (Fig.

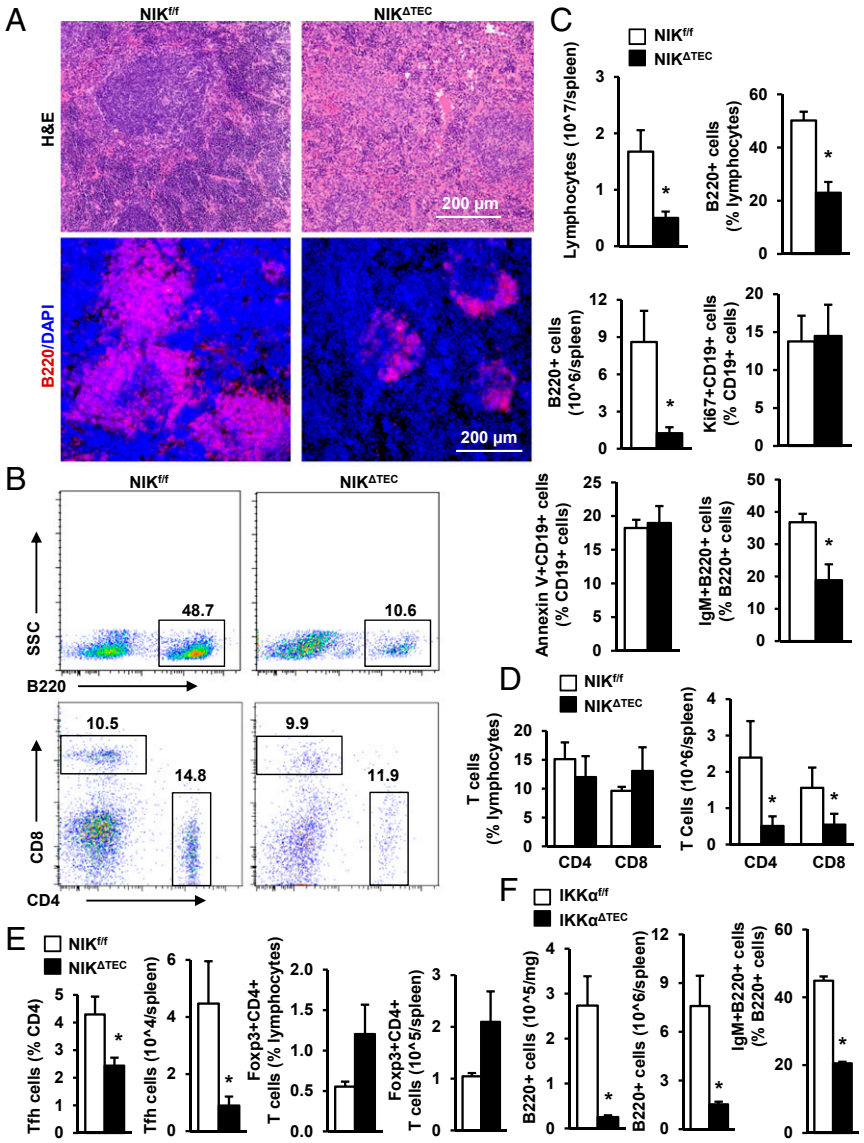

Fig. 5. NIK$^{\Delta TEC}$ and IKKα$^{\Delta TEC}$ mice have defective B cell development. (*A–E*) Lymph nodes and spleens were harvested at 10 to 15 d of age and analyzed by immunostaining or flow cytometry. (*A*) Representative spleen sections ($n = 3$). (*B*) Flow cytometric plots of spleen B cells and T cells. (The number represents percentiles.) (*C–E*) Flow cytometric assessments of spleen lymphocytes. NIK$^{\Delta TEC}$, $n = 3$ to 4; NIK$^{f/f}$, $n = 3$ to 6. (*F*) Flow cytometric assessments of spleen B cells of IKKα$^{\Delta TEC}$ ($n = 3$) and IKKα$^{f/f}$ ($n = 3$) littermates at 15 to 17 d of age. Data are presented as mean ± SEM. *$P < 0.05$, 2-tailed unpaired Student's *t* test.

6*D*), suggesting that DN differentiation is also inhibited between DN2 and DN3 stages. To gain insight into the underlying mechanism, we assessed thymocyte proliferation (Ki67 staining) and death (Annexin V staining). DN1 proliferation was higher in NIK$^{\Delta TEC}$ mice (Fig. 6*E*), likely contributing to increased DN1 frequency. DN2 proliferation was undetectable. DN3, DN4, and DP proliferations were comparable between NIK$^{\Delta TEC}$ and NIK$^{f/f}$ mice (Fig. 6*E*). DN1, DN2, DN4, and DP death was significantly higher in NIK$^{\Delta TEC}$ relative to NIK$^{f/f}$ mice (Fig. 6*E*), contributing to thymocyte reduction in NIK$^{\Delta TEC}$ mice. Notably, the number of thymic Foxp3$^+$ Treg cells was lower in NIK$^{\Delta TEC}$ mice (Fig. 6*F*). To exclude the possibility that the observed thymic phenotypes might be caused nonspecifically by sickness, we examined NIK$^{\Delta TEC}$ pups at 10 d of age when body weight and blood glucose were slightly reduced (*SI Appendix*, Fig. S7*A*). Thymic development was similarly impaired in these NIK$^{\Delta TEC}$ pups (*SI Appendix*, Fig. S7 *B* and *C*). The spleens of NIK$^{\Delta TEC}$ mice were also deficient of B cells (*SI Appendix*, Fig. S7*D*). Collectively, these results indicate that in addition to promoting negative selection, TEC-intrinsic NIK pathways are also involved in the regulation of thymocyte expansion and positive selection.

NIK and IKKα Pathways Directly Promote TEC Precursor Proliferation and mTEC Expansion. We next sought to interrogate the mechanism by which NIK/IKKα pathways regulate TEC development. Remarkably, thymic medulla were absent in NIK$^{\Delta TEC}$ mice (Fig. 7*A* and *SI Appendix*, Fig. S7*E*). Mature mTECs were also undetectable in NIK$^{\Delta TEC}$ mice, as assessed using antibodies against autoimmune regulator (Aire), keratin 5 (K5), and ulex europeus agglutinin-1 (UEA-1) (Fig. 7*A*). We next assessed TEC progenitor cells using flow cytometry (Fig. 7*B*). The frequencies of mTECs (CD45$^-$EpCAM$^+$CD205$^-$Cld4$^+$) but not cTECs (CD45$^-$EpCAM$^+$CD205$^+$Cld4$^-$) were markedly lower in NIK$^{\Delta TEC}$ than in NIK$^{f/f}$ mice (Fig. 7*C*). The numbers of mTECs, cTECs, and total TECs were also significantly lower in NIK$^{\Delta TEC}$ mice (Fig. 7 *D* and *E*). The frequencies of mTEC and activated cTECs [i.e., major

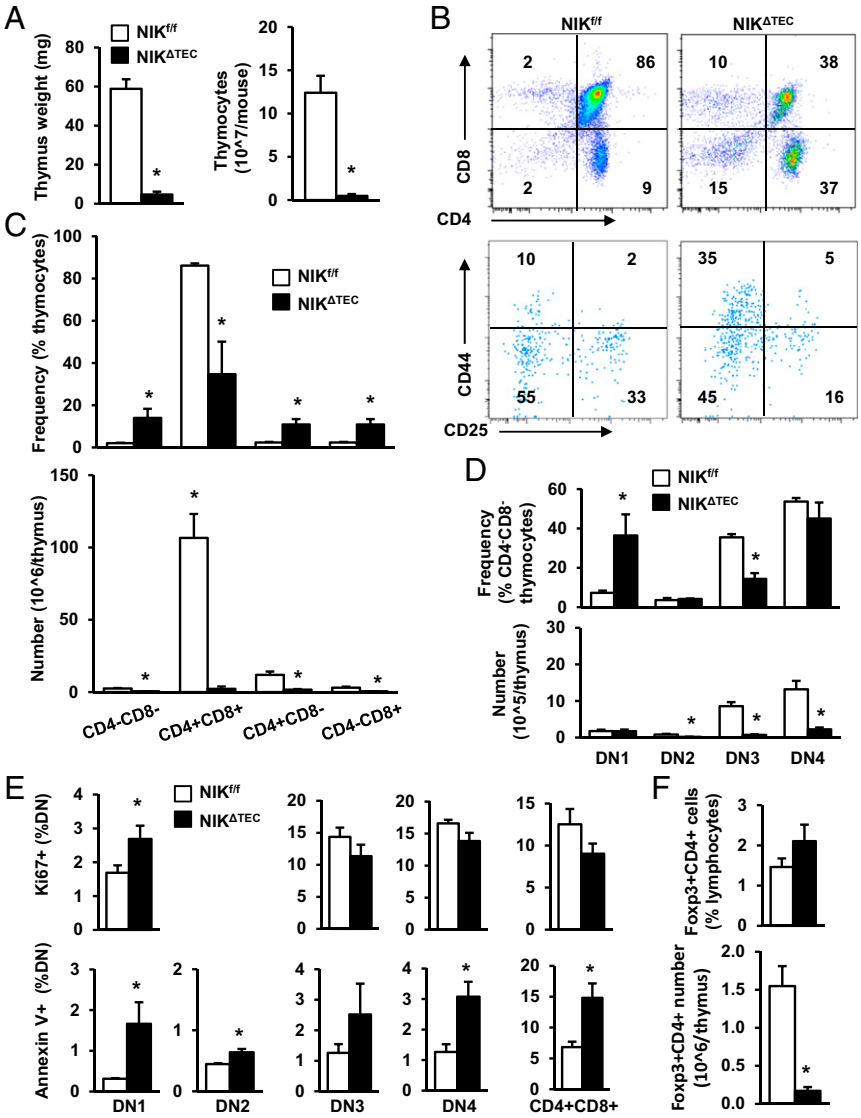

Fig. 6. NIK$^{\Delta TEC}$ mice have defective thymocyte development. Thymi were isolated from NIK$^{\Delta TEC}$ ($n = 3$ to 4) and NIK$^{f/f}$ ($n = 3$ to 6) males at 10 to 15 d of age. (*A*) Thymus weight and thymocyte number. (*B*) Flow cytometric plots of thymocytes. (The number represents percentiles.) (*C* and *D*) Flow cytometric assessments of thymocytes. (*E*) Proliferation and death of DN and DP thymocytes. (*F*) Flow cytometric assessments of thymic Treg cells. Data are presented as mean ± SEM. *$P < 0.05$, 2-tailed unpaired Student's *t* test.

histocompatibility complex (MHC) II^{high}, RANK^{high}, and CD40^{high} cells] were significantly lower in NIK$^{\Delta TEC}$ relative to NIK$^{f/f}$ mice (Fig. 7 *C* and *F*). These results indicate that cTEC development is also impaired in NIK$^{\Delta TEC}$ mice, contributing to suppression of cortical thymocyte development.

To further interrogate the mechanism responsible for mTEC deficiency in NIK$^{\Delta TEC}$ mice, we assessed bipotent (CD45$^-$EpCAM$^+$ Sca1$^+$CD49f$^+$MHC II^{low}) and mTEC lineage-committed precursors (CD45$^-$EpCAM$^+$CD205$^-$Cld4$^+$MHC II$^-$) using flow cytometry (18, 21–25). The numbers of both bipotent and mTEC lineage-committed precursors were substantially lower in NIK$^{\Delta TEC}$ relative to NIK$^{f/f}$ mice (Fig. 7 *G* and *H*). Furthermore, mTEC precursor proliferation, but not death, was significantly lower in NIK$^{\Delta TEC}$ than in NIK$^{f/f}$ mice (Fig. 7*I*). In contrast, the proliferation and death rates of cTEC precursors (CD45$^-$EpCAM$^+$ CD205$^+$Cld4$^-$MHC II$^-$) were comparable between NIK$^{\Delta TEC}$ and NIK$^{f/f}$ mice (*SI Appendix*, Fig. S8*A*). Taken together, these results suggest that NIK pathways cell-autonomously support the proliferation of bipotent and mTEC-committed precursors, thereby promoting thymic medullary development and establishment of central tolerance.

IKKα$^{\Delta TEC}$ mice, like NIK$^{\Delta TEC}$ mice, also displayed severe thymic atrophy (markedly reduced thymus weight and thymocyte number) (*SI Appendix*, Fig. S8*B*) and completely lacked thymic medulla and Aire$^+$, K5$^+$, and UEA-1$^+$ mTECs (*SI Appendix*, Fig. S8*C*). The numbers of developing thymocytes (e.g., DN1, DN2, DN3, DN4, DP), and CD4 and CD8 T cells were also significantly lower in IKKα$^{\Delta TEC}$ mice relative to IKKα$^{f/f}$ littermates (*SI Appendix*, Fig. S8 *D* and *E*). These results suggest that IKKα acts downstream of NIK to promote TEC growth and maturation and thymic T cell development.

Discussion

NIK has been extensively studied for its ability to activate the noncanonical NF–κB2 pathway. Using loss-of-function mutation (*aly*/*aly*) and global knockout mouse models, NIK was found to be required for peripheral lymph organ development (26–28). NIK-deficient thymus grafts cause autoimmune disorders in

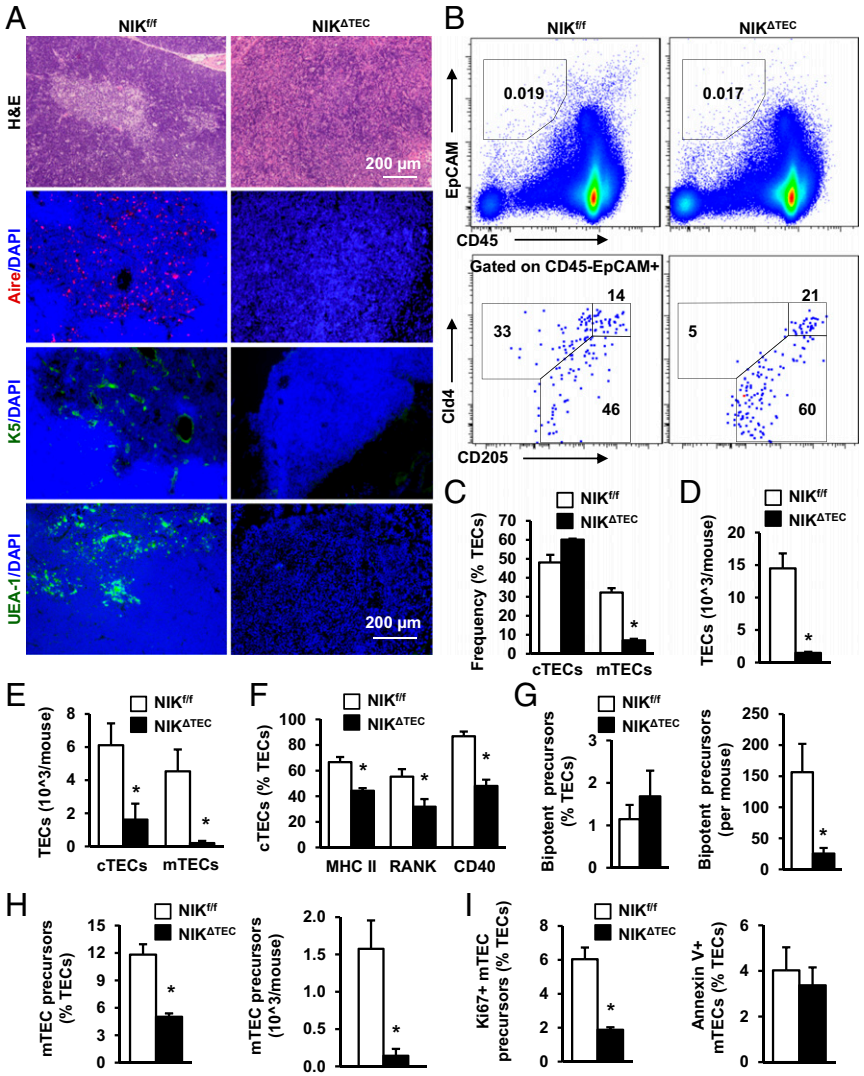

Fig. 7. NIK deficiency impairs TEC development. (*A*) Representative thymic sections at 15 to 17 d of age ($n = 4$ per group). (*B*) Flow cytometric plots of TECs. (Numbers represent percentiles.) (*C–I*) Flow cytometric assessments of cTECs, mTECs, and their precursors at 10 d of age. $NIK^{\Delta TEC}$ ($n = 3$) and $NIK^{f/f}$ ($n = 3$ to 4). Data are presented as mean ± SEM. $^*P < 0.05$, 2-tailed unpaired Student's *t* test.

recipient mice (11, 12), indicating that thymic NIK is required for suppression of autoimmunity. However, NIK target cells in the thymus are undefined. In this study, we identified TECs as critical endogenous targets of NIK and IKKα pathways, using $NIK^{\Delta TEC}$ and $IKK\alpha^{\Delta TEC}$ mice.

We found that $NIK^{\Delta TEC}$ and $IKK\alpha^{\Delta TEC}$ mice died prematurely within 18 d of age. Of note, a human homozygous loss-of-function $NIK^{Pro565Arg}$ variant is also linked to child death (13). A homozygous $NIK^{Val345Met}$ variant is associated with severe child illness (14). Thus, TEC-intrinsic NIK/IKKα pathways crucially support life in both mice and humans. Strikingly, $NIK^{\Delta TEC}$ and $IKK\alpha^{\Delta TEC}$ mice developed severe T cell-triggered inflammation, injury, and fibrosis in lungs and livers, leading to neonatal death. These findings unravel previously unrecognized TEC–liver and TEC–lung axes that critically promote liver and lung diseases, respectively.

We provided multiple lines of evidence showing that mTEC-intrinsic NIK/IKKα pathways pivotally support thymic medullary development and negative selection. $NIK^{\Delta TEC}$ and $IKK\alpha^{\Delta TEC}$ mice lacked medulla and mature mTECs expressing Aire, UEA-1, and K5. Deficiency of mTECs led to breakdown of central tolerance and production of autoreactive T cells in $NIK^{\Delta TEC}$ and $IKK\alpha^{\Delta TEC}$ mice. Consequently, $NIK^{\Delta TEC}$ and $IKK\alpha^{\Delta TEC}$ mice developed severe autoimmune liver and lung diseases, resulting in premature death. mTECs arise from both bipotent and mTEC-committed precursors (18, 21–24). Ablation of TEC NIK markedly decreased the numbers of both bipotent and mTEC-committed precursors, at least in part by inhibiting precursor proliferation. Of note, developing thymocytes secrete RANKL, CD40L, and LTβ that promote mTEC growth, differentiation, and maturation (5–7). TEC-intrinsic NIK/IKKα pathways likely mediate these cytokine signaling, thereby supporting mTEC growth and differentiation and mTEC-controlled central tolerance.

$NIK^{\Delta TEC}$ and $IKK\alpha^{\Delta TEC}$ mice displayed profound defects in cortical thymocyte development and peripheral B cell development. The numbers of DN2, DN3, DN4, and DP thymocytes were dramatically lower in $NIK^{\Delta TEC}$ and $IKK\alpha^{\Delta TEC}$ mice. Thymocyte development arrested between DN1 and DN2 stages and between DN2 and DN3 stages. Of note, cTEC activities, as assessed by expression of MHC II, RANK, and CD40, were impaired in $NIK^{\Delta TEC}$ mice, raising the possibility that cTEC-intrinsic NIK/IKKα pathways may be involved in promoting double-negative thymocyte growth and differentiation and positive selection. It is worth mentioning that during preparation of this work,

TEC-specific *NIK* knockout mice were described by another group (29), but αβ T cells, TECs, livers, and lungs were not examined. We also found that $NIK^{\Delta TEC}$ and $IKK\alpha^{\Delta TEC}$ mice lacked lymphoid follicles and germinal centers in spleens and lymph nodes. Consistently, these mice had markedly reduced B cells in their spleens and lymph nodes. Spleen Tfh cell number was reduced in $NIK^{\Delta TEC}$ and $IKK\alpha^{\Delta TEC}$ mice, raising the possibility that TEC-intrinsic NIK/IKKα pathways may stimulate commitments of thymocytes to Tfh and/or related CD4 T-lineage cells that in turn promote peripheral B cell development.

In conclusion, we have identified TEC NIK and IKKα as essential regulators of TEC development and T cell central tolerance. Inactivation of TEC-intrinsic NIK/IKKα pathways alone is sufficient to pathogenically activate autoimmunity, leading to fatal autoimmune liver disease and lung disease. The thymic NIK/IKKα pathways may serve as a potential therapeutic target for the treatment of autoimmune diseases, including chronic liver and lung diseases.

Materials and Methods

Animals. Animal experiments were conducted following the protocols approved by the University of Michigan Institutional Animal Care and Use Committee (IACUC). $NIK^{f/f}$, $IKK\alpha^{f/f}$, and Foxn1–Cre mice (C57BL/6 background) were characterized previously (15–17). Mice were housed on a 12-h light–dark cycle and fed a normal chow diet (9% fat; Lab Diet, St. Louis, MO) ad libitum with free access to water.

Blood Analysis. Blood glucose and ALT activity were measured using glucometers (Bayer Corp., Pittsburgh, PA) and an ALT reagent set (Pointe Scientific Inc., Canton, MI), respectively (30).

Immunoblotting and Immunostaining. Tissue samples were homogenized in lysis buffer (50 mM Tris, pH 7.5, 1% Nonidet P-40, 150 mM NaCl, 2 mM EGTA, 1 mM Na_3VO_4, 100 mM NaF, 10 mM $Na_4P_2O_7$, 1 mM benzamidine, 10 μg/mL aprotinin, 10 μg/mL leupeptin; 1 mM phenylmethylsulfonyl fluoride), resolved by SDS/PAGE, and immunoblotted as described previously (12). Tissue-frozen sections were prepared using a Leica cryostat (Leica Biosystems Nussloch GmbH, Nussloch, Germany), fixed in 4% paraformaldehyde, blocked with 5% normal goat serum (Life Technologies) supplemented with 1% BSA, and incubated with antibodies at 4 °C overnight. Antibodies were listed in *SI Appendix*, Table S1.

Hematoxylin and Eosin, Sirius Red Staining, and TUNEL Assays. Tissue paraffin sections were stained with hematoxylin and eosin (H&E) or 0.1% Sirius-red (Sigma, 365548) and 0.1% Fast-green (Sigma, F7252) as described previously (12). Tissue-frozen sections were fixed with 4% paraformaldehyde and then subjected to TUNEL assays using an In Situ Cell Death Detection Kit (Roche Diagnostics, Indianapolis, IN, 11684817910).

Flow Cytometry. We followed similar methods described previously (12) and in *SI Appendix*.

Thymic Epithelial Cell Isolation. Thymi were isolated, minced, and incubated at 37 °C for 40 min in PBS buffer supplemented with collagenase D (1 mg/mL) and Dispase II (1 mg/mL). Adjacent tissues were removed prior to collagenase treatment. Thymic epithelial cells were enriched on a discontinuous Percoll density gradient (densities 1.07, 1.05, and 1.01) and subjected to flow cytometric analysis.

Statistical Analysis. Data were presented as means ± SEM. Differences between groups were analyzed with 2-tailed Student's t test. $P < 0.05$ was considered statistically significant.

ACKNOWLEDGMENTS. We thank Drs. Lin Jiang, Yan Liu, Mark J. Canet, and Lei Yin for assistance and discussion. This study was supported by Grants RO1 DK115646, RO1 DK114220, and R21 AA025945 (to L.R.). L.Q. (DK105393), M.B.O. (DK47918) and Y.M.S. (CA148828) were supported by NIH grants. This work utilized the cores supported by the Michigan Diabetes Research and Training Center (NIH DK20572), the University of Michigan's Cancer Center (NIH CA46592), and the University of Michigan Gut Peptide Research Center (NIH DK34933).

1. O. Le Rouzic *et al.*, Th17 cytokines: Novel potential therapeutic targets for COPD pathogenesis and exacerbations. *Eur. Respir. J.* **50**, 1602434 (2017).
2. K. Tsuneyama *et al.*, Autoimmune features in metabolic liver disease: A single-center experience and review of the literature. *Clin. Rev. Allergy Immunol.* **45**, 143–148 (2013).
3. S. Sutti, S. Bruzzì, E. Albano, The role of immune mechanisms in alcoholic and non-alcoholic steatohepatitis: A 2015 update. *Expert Rev. Gastroenterol. Hepatol.* **10**, 243–253 (2016).
4. L. Klein, B. Kyewski, P. M. Allen, K. A. Hogquist, Positive and negative selection of the T cell repertoire: What thymocytes see (and don't see). *Nat. Rev. Immunol.* **14**, 377–391 (2014).
5. Y. Hikosaka *et al.*, The cytokine RANKL produced by positively selected thymocytes fosters medullary thymic epithelial cells that express autoimmune regulator. *Immunity* **29**, 438–450 (2008).
6. T. Boehm, S. Scheu, K. Pfeffer, C. C. Bleul, Thymic medullary epithelial cell differentiation, thymocyte emigration, and the control of autoimmunity require lympho-epithelial cross talk via LTbetaR. *J. Exp. Med.* **198**, 757–769 (2003).
7. T. Akiyama *et al.*, The tumor necrosis factor family receptors RANK and CD40 cooperatively establish the thymic medullary microenvironment and self-tolerance. *Immunity* **29**, 423–437 (2008).
8. J. A. Williams *et al.*, Thymic medullary epithelium and thymocyte self-tolerance require cooperation between CD28-CD80/86 and CD40-CD40L costimulatory pathways. *J. Immunol.* **192**, 630–640 (2014).
9. S. R. Jenkinson *et al.*, TRAF3 enforces the requirement for T cell cross-talk in thymic medullary epithelial development. *Proc. Natl. Acad. Sci. U.S.A.* **110**, 21107–21112 (2013).
10. S. C. Sun, The noncanonical NF-κB pathway. *Immunol. Rev.* **246**, 125–140 (2012).
11. F. Kajiura *et al.*, NF-kappa B-inducing kinase establishes self-tolerance in a thymic stroma-dependent manner. *J. Immunol.* **172**, 2067–2075 (2004).
12. H. Shen *et al.*, Thymic NF-kappaB-inducing kinase (NIK) regulates CD4+ T cell-elicited liver injury and fibrosis in mice. *J. Hepatol.* **67**, 100–109 (2017).
13. K. L. Willmann *et al.*, Biallelic loss-of-function mutation in NIK causes a primary immunodeficiency with multifaceted aberrant lymphoid immunity. *Nat. Commun.* **5**, 5360 (2014).
14. N. Schlechter *et al.*, Exome sequencing identifies a novel *MAP3K14* mutation in recessive atypical combined immunodeficiency. *Front. Immunol.* **8**, 1624 (2017).
15. J. Gordon *et al.*, Specific expression of lacZ and cre recombinase in fetal thymic epithelial cells by multiplex gene targeting at the Foxn1 locus. *BMC Dev. Biol.* **7**, 69 (2007).
16. Y. Liu *et al.*, Liver NF-kappaB-inducing kinase (NIK) promotes liver steatosis and glucose counterregulation in male mice with obesity. *Endocrinology* **158**, 1207–1216 (2017).
17. B. Liu *et al.*, IKKalpha is required to maintain skin homeostasis and prevent skin cancer. *Cancer Cell* **14**, 212–225 (2008).
18. C. C. Bleul *et al.*, Formation of a functional thymus initiated by a postnatal epithelial progenitor cell. *Nature* **441**, 992–996 (2006).
19. C. S. Nowell *et al.*, Foxn1 regulates lineage progression in cortical and medullary thymic epithelial cells but is dispensable for medullary sublineage divergence. *PLoS Genet.* **7**, e1002348 (2011).
20. H. Hu *et al.*, Noncanonical NF-kappaB regulates inducible costimulator (ICOS) ligand expression and T follicular helper cell development. *Proc. Natl. Acad. Sci. U.S.A.* **108**, 12827–12832 (2011).
21. S. W. Rossi, W. E. Jenkinson, G. Anderson, E. J. Jenkinson, Clonal analysis reveals a common progenitor for thymic cortical and medullary epithelium. *Nature* **441**, 988–991 (2006).
22. S. Ulyanchenko *et al.*, Identification of a bipotent epithelial progenitor population in the adult thymus. *Cell Rep.* **14**, 2819–2832 (2016).
23. M. Sekai, Y. Hamazaki, N. Minato, Medullary thymic epithelial stem cells maintain a functional thymus to ensure lifelong central T cell tolerance. *Immunity* **41**, 753–761 (2014).
24. I. Ohigashi *et al.*, Adult thymic medullary epithelium is maintained and regenerated by lineage-restricted cells rather than bipotent progenitors. *Cell Rep.* **13**, 1432–1443 (2015).
25. K. Wong *et al.*, Multilineage potential and self-renewal define an epithelial progenitor cell population in the adult thymus. *Cell Rep.* **8**, 1198–1209 (2014).
26. S. Miyawaki *et al.*, A new mutation, aly, that induces a generalized lack of lymph nodes accompanied by immunodeficiency in mice. *Eur. J. Immunol.* **24**, 429–434 (1994).
27. R. Koike *et al.*, The splenic marginal zone is absent in alymphoplastic aly mutant mice. *Eur. J. Immunol.* **26**, 669–675 (1996).
28. L. Yin *et al.*, Defective lymphotoxin-beta receptor-induced NF-kappaB transcriptional activity in NIK-deficient mice. *Science* **291**, 2162–2165 (2001).
29. F. Mair *et al.*, The NFκB-inducing kinase is essential for the developmental programming of skin-resident and IL-17-producing γδ T cells. *ELife* **4**, e10087 (2015).
30. H. Shen *et al.*, Mouse hepatocyte overexpression of NF-κB-inducing kinase (NIK) triggers fatal macrophage-dependent liver injury and fibrosis. *Hepatology* **60**, 2065–2076 (2014).